J|A|C|S ARTICLES

Published on Web 10/11/2010

Context-Dependent Effects of Asparagine Glycosylation on Pin WW Folding Kinetics and Thermodynamics

Joshua L. Price,[†] Dalit Shental-Bechor,[‡] Apratim Dhar,[§] Maurice J. Turner,[†] Evan T. Powers,[†] Martin Gruebele,[#] Yaakov Levy,[*,‡] and Jeffery W. Kelly[*,†]

Departments of Chemistry and Molecular and Experimental Medicine and The Skaggs Institute for Chemical Biology, The Scripps Research Institute, La Jolla, California 92037, United States, Department of Structural Biology, Weizmann Institute of Science, Rehovot 76100, Israel, and Center for Biophysics and Computational Biology and Departments of Chemistry and Physics, University of Illinois, Urbana, Illinois 61801, United States

Received August 2, 2010; E-mail: jkelly@scripps.edu; koby.levy@weizmann.ac.il

Abstract: Asparagine glycosylation is one of the most common and important post-translational modifications of proteins in eukaryotic cells. *N*-Glycosylation occurs when a triantennary glycan precursor is transferred en bloc to a nascent polypeptide (harboring the N−X−T/S sequon) as the peptide is cotranslationally translocated into the endoplasmic reticulum (ER). In addition to facilitating binding interactions with components of the ER proteostasis network, *N*-glycans can also have intrinsic effects on protein folding by directly altering the folding energy landscape. Previous work from our laboratories (Hanson et al. *Proc. Natl. Acad. Sci. U.S.A.* **2009**, *109*, 3131−3136; Shental-Bechor, D.; Levy, Y. *Proc. Natl. Acad. Sci. U.S.A.* **2008**, *105*, 8256−8261) suggested that the three sugar residues closest to the protein are sufficient for accelerating protein folding and stabilizing the resulting structure in vitro; even a monosaccharide can have a dramatic effect. The highly conserved nature of these three proximal sugars in *N*-glycans led us to speculate that introducing an *N*-glycosylation site into a protein that is not normally glycosylated would stabilize the protein and increase its folding rate in a manner that does not depend on the presence of specific stabilizing protein−saccharide interactions. Here, we test this hypothesis experimentally and computationally by incorporating an N-linked GlcNAc residue at various positions within the Pin WW domain, a small β-sheet-rich protein. The results show that an increased folding rate and enhanced thermodynamic stability are not general, context-independent consequences of *N*-glycosylation. Comparison between computational predictions and experimental observations suggests that generic glycan-based excluded volume effects are responsible for the destabilizing effect of glycosylation at highly structured positions. However, this reasoning does not adequately explain the observed destabilizing effect of glycosylation within flexible loops. Our data are consistent with the hypothesis that specific, evolved protein−glycan contacts must also play an important role in mediating the beneficial energetic effects on protein folding that glycosylation can confer.

Introduction

Approximately one-third of the human proteome is folded in the endoplasmic reticulum (ER),[1] where most of these proteins are cotranslationally *N*-glycosylated. In eukaryotes, *N*-glycosylation is catalyzed by the oligosaccharyltransferase enzyme complex (OST), which transfers the conserved triantennary *N*-glycan precursor ($Glc_3Man_9GlcNAc_2$) en bloc to the side-chain amide N of an Asn residue within the recognition sequence, Asn−Xxx−Thr/Ser, known as the *N*-glycosylation "sequon" (Figure 1).[2−4] The outer two Glc residues from the A-branch of the conserved triantennary glycan precursor are rapidly removed by glucosidase I and glucosidase II, thereby enabling the nascent chain of the glycoprotein to enter the calnexin and calreticulin (CNX/CRT)-assisted folding cycle in the ER,[5,6] part of the ER proteostasis network.[7−9] In this way, *N*-glycosylation has an extrinsic effect on protein folding, trafficking, and function.[9,10]

Removal of the third Glc on the A branch of the glycan precursor ablates binding of the glycoprotein to CNX/CRT and allows the glycoprotein to exit the CNX/CRT cycle.[6] Properly folded glycoproteins can then engage trafficking receptors and

[†] The Scripps Research Institute.
[‡] Weizmann Institute of Science.
[§] Department of Chemistry, University of Illinois.
[#] Center for Biophysics and Computational Biology and Departments of Chemistry and Physics, University of Illinois.

(1) Huh, W.-K.; Falvo, J. V.; Gerke, L. C.; Carroll, A. S.; Howson, R. W.; Weissman, J. S.; O'Shea, E. K. *Nature* **2003**, *425*, 686–691.
(2) Kornfeld, R.; Kornfeld, S. *Annu. Rev. Biochem.* **1985**, *54*, 631–664.
(3) Yan, A.; Lennarz, W. J. *J. Biol. Chem.* **2005**, *280*, 3121–3124.
(4) Kelleher, D. J.; Gilmore, R. *Glycobiology* **2006**, *16*, 47R–62R.
(5) Helenius, A.; Aebi, M. *Science* **2001**, *291*, 2364–2369.
(6) Molinari, M. *Nat. Chem. Biol.* **2007**, *3*, 313–320.
(7) Balch, W. E.; Morimoto, R. I.; Dillin, A.; Kelly, J. W. *Science* **2008**, *319*, 916–919.
(8) Powers, E. T.; Morimoto, R. I.; Dillin, A.; Kelly, J. W.; Balch, W. E. *Annu. Rev. Biochem.* **2009**, *78*, 959–991.
(9) Ong, D. S. T.; Mu, T.-W.; Palmer, A. E.; Kelly, J. W. *Nat. Chem. Biol.* **2010**, *6*, 424–432.
(10) Parthasarathy, R.; Subramanian, S.; Boder, E. T.; Discher, D. E. *Biotechnol. Bioeng.* **2006**, *93*, 159–168.

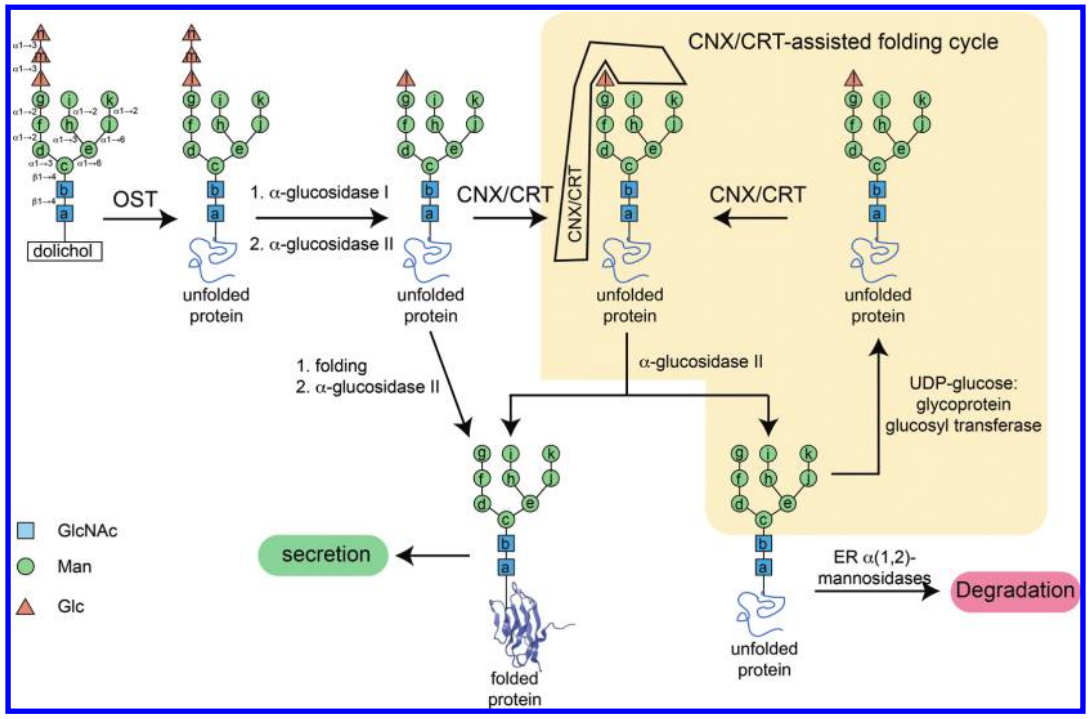

Figure 1. Extrinsic effects of *N*-glycosylation: *N*-glycosylation allows a glycoprotein to enter the calnexin/calreticulin-assisted folding cycle in the ER, which allows it to fold and be secreted or to be targeted for degradation if attempts at proper folding are unsuccessful.

be exported from the ER by vesicular trafficking.[11−13] The ER folding sensor UDP-glucose:glycoprotein glucosyltransferase detects and reglucosylates misfolded proteins,[14−17] allowing them to re-enter the CNX/CRT cycle, which provides another chance to acquire the proper fold. Glycoproteins that persistently fail to fold properly eventually encounter ER-resident α(1−2)-mannosidases,[18] which remove α(1,2)-mannose residues from the branches of the triantennary glycan precursor, thereby reducing the ability of the glycoprotein to re-enter the CNX/CRT cycle[19,20] and ultimately allowing it to be targeted it for proteasomal degradation in the cytosol via processes involving dislocation from the ER to the cytosol and ubiquitination (Figure 1).[18,21,22]

The triantennary glycan precursors on folded glycoproteins are extensively remodeled in the Golgi,[2] which vastly expands the functional repertoire of the proteome, for example, by enabling binding interactions within and especially outside of the cell. While much is known about how *N*-glycans mediate extrinsic biologically assisted glycoprotein folding or degradation through binding interactions (an area of continuing investigation),[5,23] considerably less is known about the intrinsic or chemical basis for why so many eukaryotic proteins are *N*-glycosylated.

Several researchers have suggested that glycans play an intrinsic role in (1) stabilizing protein structure,[24] (2) accelerating folding,[25] (3) promoting the formation of secondary structure,[26−41]

(11) Gürkan, C.; Stagg, S. M.; LaPointe, P.; Balch, W. E. *Nat. Rev. Mol. Cell Biol.* **2006**, *7*, 727–738.
(12) Sekijima, Y.; Wiseman, R. L.; Matteson, J.; Hammarström, P.; Miller, S. R.; Sawkar, A. R.; Balch, W. E.; Kelly, J. W. *Cell* **2005**, *121*, 73–85.
(13) Wiseman, R. L.; Powers, E. T.; Buxbaum, J. N.; Kelly, J. W.; Balch, W. E. *Cell* **2007**, *131*, 809–821.
(14) Caramelo, J. J.; Castro, O. A.; de Prat-Gay, G.; Parodi, A. J. *J. Biol. Chem.* **2004**, *279*, 46280–46285.
(15) Taylor, S. C.; Ferguson, A. D.; Bergeron, J. J. M.; Thomas, D. Y. *Nat. Struct. Mol. Biol.* **2004**, *11*, 128–134.
(16) Molinari, M.; Galli, C.; Vanoni, O.; Arnold, S. M.; Kaufman, R. J. *Mol. Cell* **2005**, *20*, 503–512.
(17) Ritter, C.; Quirin, K.; Kowarik, M.; Helenius, A. *EMBO J.* **2005**, *24*, 1730–1738.
(18) Lederkremer, G. Z.; Glickman, M. H. *Trends Biochem. Sci.* **2005**, *30*, 297–303.
(19) Sousa, M. C.; Ferrero-Garcia, M. A.; Parodi, A. J. *Biochemistry* **1992**, *31*, 97–105.
(20) Spiro, R. G.; Zhu, Q.; Bhoyroo, V.; Söling, H.-D. *J. Biol. Chem.* **1996**, *271*, 11588–11594.
(21) Cabral, C. M.; Liu, Y.; Sifers, R. N. *Trends Biochem. Sci.* **2001**, *26*, 619–624.
(22) Moremen, K. W.; Molinari, M. *Curr. Opin. Chem. Biol.* **2006**, *16*, 592–599.
(23) Varki, A. *Glycobiology* **1993**, *3*, 97–130.
(24) Wormald, M. R.; Dwek, R. A. *Struct. Fold. Des.* **1999**, *7*, R155–R160.
(25) Yamaguchi, H. *Trends Glycosci. Glycotechnol.* **2002**, *14*, 139–151.
(26) Wormald, M. R.; Wooten, E. W.; Bazzo, R.; Edge, C. J.; Feinstein, A.; Rademacher, T. W.; Dwek, R. A. *Eur. J. Biochem.* **1991**, *198*, 131–139.
(27) Laszlo, O., Jr.; Jan, T.; Emma, K.; Laszlo, U.; Henry, H. M.; Miklos, H. *Int. J. Pept. Protein Res.* **1991**, *38*, 476–482.
(28) Laczko, I.; Hollosi, M.; Urge, L.; Ugen, K. E.; Weiner, D. B.; Mantsch, H. H.; Thurin, J.; Otvos, L. *Biochemistry* **1992**, *31*, 4282–4288.
(29) Urge, L.; Gorbics, L.; Otvos, L., Jr. *Biochem. Biophys. Res. Commun.* **1992**, *184*, 1125–1132.
(30) Andreotti, A. H.; Kahne, D. *J. Am. Chem. Soc.* **1993**, *115*, 3352–3353.
(31) Liang, R.; Andreotti, A. H.; Kahne, D. *J. Am. Chem. Soc.* **1995**, *117*, 10395–10396.
(32) Rickert, K. W.; Imperiali, B. *Chem. Biol.* **1995**, *2*, 751–759.
(33) Imperiali, B.; Rickert, K. W. *Proc. Natl. Acad. Sci. U.S.A.* **1995**, *92*, 97–101.
(34) Live, D. H.; Kumar, R. A.; Beebe, X.; Danishefsky, S. J. *Proc. Natl. Acad. Sci. U.S.A.* **1996**, *93*, 12759–12761.
(35) O'Connor, S. E.; Imperiali, B. *Chem. Biol.* **1996**, *3*, 803–812.
(36) O'Connor, S. E.; Imperiali, B. *J. Am. Chem. Soc.* **1997**, *119*, 2295–2296.
(37) O'Connor, S. E.; Imperiali, B. *Chem. Biol.* **1998**, *5*, 427–437.
(38) Imperiali, B.; O'Connor, S. E. *Curr. Opin. Chem. Biol.* **1999**, *3*, 643–649.
(39) O'Connor, S. E.; Pohlmann, J.; Imperiali, B.; Saskiawan, I.; Yamamoto, K. *J. Am. Chem. Soc.* **2001**, *123*, 6187–6188.

(4) reducing aggregation, possibly by shielding hydrophobic surfaces,[25,42,43] and (5) increasing folding cooperativity,[42] all through built-in mechanisms. That glycans can play such intrinsic roles is further supported by evidence that the *N*-glycan alone can rescue protein folding in cells when CNX/CRT are absent or nonfunctional or when the *N*-glycan itself is truncated and unable to interact with CNX/CRT.[2,44]

Previous work in our laboratories[45,46] and by others[26−34,36−41,47] suggests that the first two or three sugars of an *N*-glycan (those that are directly adjacent to protein) play an intrinsic role in accelerating protein folding and stabilizing the resulting structure. Even a single N-linked *N*-acetyl-D-glucosamine (GlcNAc) residue can have a dramatic effect on protein thermodynamics and kinetics. These three proximal sugars, two GlcNAc residues followed by one D-mannose (Man) residue, form a triose core that is strictly conserved among eukaryotic *N*-glycans. The highly conserved nature of the Asn−$GlcNAc_2$Man triose led us to speculate that *N*-glycosylation might be a part of a general strategy to accelerate and stabilize protein folding intrinsically, especially in proteins where the sequence required for function might be at odds with optimal folding energetics.[45]

We hypothesized that *N*-glycosylation of a naïve protein (i.e., one that is not normally glycosylated) would destabilize the denatured ensemble of the protein relative to the native state (by restricting the conformational entropy of the denatured ensemble,[26,32,34,36,37,39,48] and/or by blocking residual enthalpically favorable interactions[46]), thus increasing the folding rate and thermodynamic stability of the glycoprotein relative to the nonglycosylated protein. We expected this effect to be general and independent of specific interactions between the oligosaccharide and protein side-chain or backbone groups.[45] Recent theoretical work supports this hypothesis: the glycosylation-naïve Src SH3 domain is generally stabilized by the addition of a model glycan in native topology-based simulations, provided that the glycan is not appended to a highly structured position.[46,49] The model glycan in these simulations was an entropic chain that can only have generic excluded volume effects on the protein, suggesting that glycosylation can stabilize proteins without requiring specific favorable protein−oligosaccharide interactions. However, the simulations also indicate that glycan-based excluded volume effects are not universally stabilizing. The flexibility and structural characteristics of the glycosylation site can have a substantial impact: at positions involved in α-helical or β-sheet secondary structure, glycosylation tends to destabilize the protein, presumably because the bulky glycan disrupts important native state interactions.

Here, we describe an experimental and computational study in which we have employed a WW domain protein to decipher the effect that glycosylation has on protein folding thermodynamics and kinetics. The WW domain of human Pin 1 (Pin WW) is a β-sheet protein in which three antiparallel β-strands are connected by two loops, with loop 1 connecting β-strands 1 and 2 and loop 2 connecting β-strands 2 and 3 (Figure 2A,C).[50−52] The folding kinetics and thermodynamics of Pin WW have been characterized extensively.[51,53−69] Pin WW is relatively stable ($T_m = 57.5$ °C, see Table 1), tolerates mutations at most of its 34 residues, and is naïve to glycosylation (as a domain in a cytosolic protein, Pin WW is not normally glycosylated). Importantly, the short length of the Pin WW domain sequence allows us to prepare homogenously glycosylated[70] (Asn−GlcNAc) variants by solid-phase peptide synthesis.[71−73] The results of the Asn−GlcNAc scan through the Pin WW domain demonstrate that an increased folding rate and enhanced thermodynamic stabilization are not general, context-independent consequences of *N*-glycosylation. In the rare cases where stabilization was observed in the Pin WW domain as a result of Asn−GlcNAc incorporation, the magnitude was 20-fold less than what was observed upon the addition of a GlcNAc residue to the β-sheet-rich human glycoprotein CD2ad, suggesting that

(40) Wormald, M. R.; Petrescu, A.-J.; Pao, Y.-L.; Glithero, A.; Elliott, T.; Dwek, R. A. *Chem. Rev.* **2002**, *102*, 371–386.
(41) Bosques, C. J.; Tschampel, S. M.; Woods, R. J.; Imperiali, B. *J. Am. Chem. Soc.* **2004**, *126*, 8421–8425.
(42) Mitra, N.; Sinha, S.; Ramya, T. N. C.; Surolia, A. *Trends Biochem. Sci.* **2006**, *31*, 156–163.
(43) Petrescu, A.-J.; Milac, A.-L.; Petrescu, S.; Dwek, R. A.; Wormald, M. R. *Glycobiology* **2004**, *14*, 103–114.
(44) Trombetta, E. S. *Glycobiology* **2003**, *13*, 77R–91R.
(45) Hanson, S. R.; Culyba, E. K.; Hsu, T.-L.; Wong, C.-H.; Kelly, J. W.; Powers, E. T. *Proc. Natl. Acad. Sci. U.S.A.* **2009**, *106*, 3131–3136.
(46) Shental-Bechor, D.; Levy, Y. *Proc. Natl. Acad. Sci. U.S.A.* **2008**, *105*, 8256–8261.
(47) Chang, V. T.; Crispin, M.; Aricescu, A. R.; Harvey, D. J.; Nettleship, J. E.; Fennelly, J. A.; Yu, C.; Boles, K. S.; Evans, E. J.; Stuart, D. I.; Dwek, R. A.; Jones, E. Y.; Owens, R. J.; Davis, S. J. *Structure* **2007**, *15*, 267–273.
(48) Reinherz, E. L.; Li, J.; Smoylar, A.; Wyss, D. F.; Knoppers, M. H.; Willis, K. J.; Arulanandam, A. R. N.; Choi, J. S.; Wagner, G. *Science* **1996**, *273*, 1242–1242.
(49) Shental-Bechor, D.; Levy, Y. *Curr. Opin. Struct. Biol.* **2009**, *19*, 524–533.
(50) Ranganathan, R.; Lu, K. P.; Hunter, T.; Noel, J. P. *Cell* **1997**, *89*, 875–886.
(51) Kowalski, J. A.; Kiu, K.; Kelly, J. W. *Biopolymers* **2002**, *63*, 111–121.
(52) Koepf, E. K.; Petrassi, H. M.; Sudol, M.; Kelly, J. W. *Protein Sci.* **1999**, *8*, 841–853.
(53) Jäger, M.; Deechongkit, S.; Koepf, E. K.; Nguyen, H.; Gao, J.; Powers, E. T.; Gruebele, M.; Kelly, J. W. *Biopolymers* **2008**, *90*, 751–758.
(54) Koepf, E. K.; Petrassi, H. M.; Ratnaswamy, G.; Huff, M. E.; Sudol, M.; Kelly, J. W. *Biochemistry* **1999**, *38*, 14338–14351.
(55) Jäger, M.; Nguyen, H.; Crane, J. C.; Kelly, J. W.; Gruebele, M. *J. Mol. Biol.* **2001**, *311*, 373–393.
(56) Kaul, R.; Angeles, A. R.; Jäger, M.; Powers, E. T.; Kelly, J. W. *J. Am. Chem. Soc.* **2001**, *123*, 5206–5212.
(57) Deechongkit, S.; Kelly, J. W. *J. Am. Chem. Soc.* **2002**, *124*, 4980–4986.
(58) Kaul, R.; Deechongkit, S.; Kelly, J. W. *J. Am. Chem. Soc.* **2002**, *124*, 11900–11907.
(59) Nguyen, H.; Jäger, M.; Moretto, A.; Gruebele, M.; Kelly, J. W. *Proc. Natl. Acad. Sci. U.S.A.* **2003**, *100*, 3948–3953.
(60) Deechongkit, S.; Nguyen, H.; Powers, E. T.; Dawson, P. E.; Gruebele, M.; Kelly, J. W. *Nature* **2004**, *430*, 101–105.
(61) Nguyen, H.; Jäger, M.; Kelly, J. W.; Gruebele, M. *J. Phys. Chem. B* **2005**, *109*, 15182–15186.
(62) Jäger, M.; Zhang, Y.; Bieschke, J.; Nguyen, H.; Dendle, M.; Bowman, M. E.; Noel, J. P.; Gruebele, M.; Kelly, J. W. *Proc. Natl. Acad. Sci. U.S.A.* **2006**, *103*, 10648–10653.
(63) Jäger, M.; Nguyen, H.; Dendle, M.; Gruebele, M.; Kelly, J. W. *Protein Sci.* **2007**, *16*, 1495–1501.
(64) Sharpe, T.; Jonsson, A. L.; Rutherford, T. J.; Daggett, V.; Fersht, A. R. *Protein Sci.* **2007**, *16*, 2233–2239.
(65) Jäger, M.; Dendle, M.; Fuller, A. A.; Kelly, J. W. *Protein Sci.* **2007**, *16*, 2306–2313.
(66) Liu, F.; Du, D.; Fuller, A. A.; Davoren, J. E.; Wipf, P.; Kelly, J. W.; Gruebele, M. *Proc. Natl. Acad. Sci. U.S.A.* **2008**, *105*, 2369–2374.
(67) Fuller, A. A.; Du, D.; Liu, F.; Davoren, J. E.; Bhabha, G.; Kroon, G.; Case, D. A.; Dyson, H. J.; Powers, E. T.; Wipf, P.; Gruebele, M.; Kelly, J. W. *Proc. Natl. Acad. Sci. U.S.A.* **2009**, *106*, 11067–11072.
(68) Jäger, M.; Dendle, M.; Kelly, J. W. *Protein Sci.* **2009**, *18*, 1806–1813.
(69) Gao, J.; Bosco, D. A.; Powers, E. T.; Kelly, J. W. *Nat. Struct. Mol. Biol.* **2009**, *16*, 684–690.
(70) Bertozzi, C. R.; Kiessling, L. L. *Science* **2001**, *291*, 2357–2364.
(71) Otvos, L., Jr.; Wroblewski, K.; Kollat, E.; Perczel, A.; Hollosi, M.; Fasman, G. D.; Ertl, H. C. J.; Thurin, J. *Pept. Res.* **1989**, *2*, 362–364.
(72) Otvos, L., Jr.; Urge, L.; Hollosi, M.; Wroblewski, K.; Graczyk, G.; Fasman, G. D.; Thurin, J. *Tetrahedron Lett.* **1990**, *31*, 5889–5892.
(73) Meldal, M.; Bock, K. *Tetrahedron Lett.* **1990**, *31*, 6987–6990.

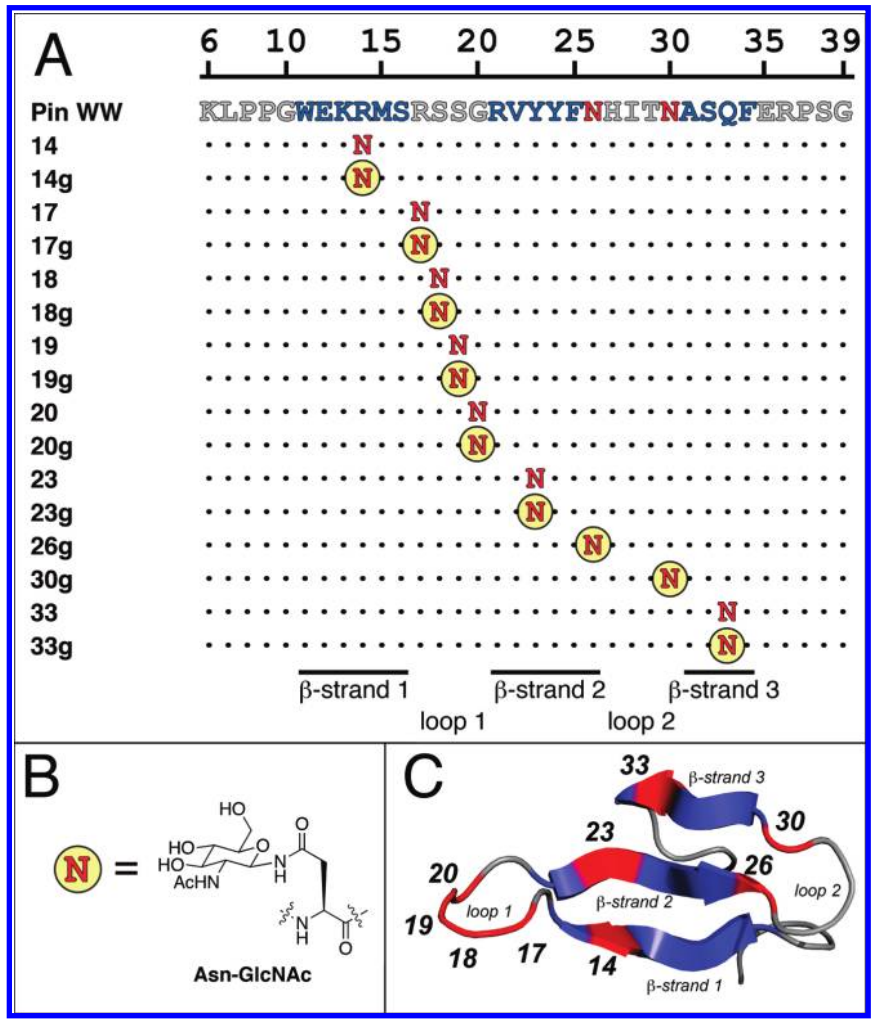

Figure 2. (A) Amino acid sequences for the parent protein, Pin WW, and 16 other variants in which residues in the parent sequence were replaced by either Asn or Asn-linked GlcNAc. (B) Structure of Asn−GlcNAc. (C) Ribbon diagram of Pin WW domain (rendered in Pymol) showing the location of the positions where Asn or Asn−GlcNAc have been incorporated (see ref 50; PDB: 1PIN).

Table 1. Experimentally Measured Melting Temperatures of Pin WW Variants with Asn or Asn−GlcNAc at the Indicated Positions with Comparisons to the Computationally Predicted Changes in Melting Temperature[a]

structural context	protein	residue at indicated position	T_m (°C)	ΔT_m (°C)	measured % change in T_m[b]	predicted % change in T_m
β-strand 1	**14**	Asn	32.1 ± 0.8	−20	−7	2.4
	14g	Asn−GlcNAc	∼10			
loop 1	**17**	Asn	54.7 ± 0.3	−0.8 ± 0.4	−0.2	3.5
	17g	Asn−GlcNAc	53.9 ± 0.3			
	18	Asn	56.0 ± 0.2	−2.4 ± 0.4	−0.7	3.1
	18g	Asn−GlcNAc	53.6 ± 0.3			
	19	Asn	56.3 ± 0.2	−2.9 ± 0.3	−0.9	4.0
	19g	Asn−GlcNAc	53.4 ± 0.3			
	20	Asn	53.0 ± 0.3	*1.8 ± 0.4*	*0.5*	*2.7*
	20g	Asn−GlcNAc	54.8 ± 0.2			
β-strand 2	**23**	Asn	30 ± 2	*−20*	*−7*	−0.5
	23g	Asn−GlcNAc	∼10			
	Pin WW	Asn	57.5 ± 0.3	*−50*	*−14*	*−2.4*
	26g	Asn−GlcNAc	∼10			
loop 2	**Pin WW**	Asn	57.5 ± 0.3	*1.3 ± 0.5*	*0.4*	*3.6*
	30g	Asn−GlcNAc	58.8 ± 0.4			
β-strand 3	**33**	Asn	40.5 ± 0.6	*−4.4 ± 1.1*	*−1.4*	*−0.8*
	33g	Asn−GlcNAc	36.1 ± 1.0			

[a] Variants for which experimental observations agree with computational predictions are italicized. Measured melting temperatures were obtained via variable temperature circular dichroism (CD) experiments on 100 μM solutions of each Pin WW domain variant in 20 mM sodium phosphate buffer (pH 7). Variable temperature CD experiments for each variant were repeated at least three times; the uncertainties in melting temperature values represent the resulting standard error in T_m (see the Supporting Information for details). [b] Percent change in melting temperature for each pair of variants was calculated using absolute melting temperatures (in K) rather than melting temperatures in °C.

Table 2. Experimentally Measured and Computationally Predicted Folding Free Energies for Pin WW Variants Having Either Asn or Asn−GlcNAc at the Indicated Positions[a]

structural context	protein	residue at indicated position	measured ΔG_f (kcal/mol)[b]	measured $\Delta\Delta G_f$ (kcal/mol)[b]	predicted $\Delta\Delta G_f$ (kcal/mol)[c]
β-strand 1	**14**	Asn	1.80 ± 0.17	−[d]	−0.30
	14g	Asn−GlcNAc	−[d]		
loop 1	**17**	Asn	0.02 ± 0.03	0.07 ± 0.05	−0.45
	17g	Asn−GlcNAc	0.10 ± 0.04		
	18	Asn	−0.10 ± 0.02	0.22 ± 0.05	−0.30
	18g	Asn−GlcNAc	0.13 ± 0.04		
	19	Asn	−0.13 ± 0.03	0.28 ± 0.05	−0.53
	19g	Asn−GlcNAc	0.15 ± 0.03		
	20	Asn	0.18 ± 0.03	*−0.16 ± 0.05*	*−0.35*
	20g	Asn−GlcNAc	0.02 ± 0.03		
β-strand 2	**23**	Asn	2.12 ± 0.28	−[d]	*0.08*
	23g	Asn−GlcNAc	−[d]		
	Pin WW	Asn	−0.25 ± 0.04	−[d]	*0.30*
	26g	Asn−GlcNAc	−[d]		
loop 2	**Pin WW**	Asn	−0.25 ± 0.04	*−0.12 ± 0.07*	*−0.60*
	30g	Asn−GlcNAc	−0.36 ± 0.05		
β-strand 3	**33**	Asn	1.24 ± 0.08	*0.31 ± 0.17*	*0.10*
	33g	Asn−GlcNAc	1.55 ± 0.15		

[a] Variants for which experimental observations agree with computational predictions are italicized. [b] Folding free energies for each Pin WW variant were derived from experimental variable temperature circular dichroism data and were calculated at 55 °C (the fit parameters used to calculate these values are given in the Supporting Information). [c] Predicted changes to folding free energy resulting from the Asn to Asn(GlcNAc) mutation at the indicated positions were calculated on the basis of the all-atom native-topology model at the calculated melting temperature of the corresponding nonglycosylated Pin WW variant (unlike the measured folding free energies, which are all at 55 °C). Uncertainties represent standard errors in each value. [d] ΔG_f and $\Delta\Delta G_f$ values for positions **14g**, **23g**, and **26g** could not be calculated because of the low thermal stability of these variants.

context-specific, evolved protein−glycan contacts play an important role in mediating the thermodynamic and kinetic effects of glycosylation on protein folding.

Results

We selected nine positions in Pin WW wherein residues in the sequence of the parent protein Pin WW were replaced with either Asn (as in proteins **14**, **17**, **18**, **19**, **20**, **23**, and **33**; note that the parent Pin WW sequence already has Asn at posititions 26 and 30) or an Asn-linked GlcNAc residue (Asn−GlcNAc, as in proteins **14g**, **17g**, **18g**, **19g**, **20g**, **23g**, **26g**, **30g**, and **33g**; see Figure 2A, where the number in the name of each protein indicates the position of the substitution, and proteins with Asn−GlcNAc at these positions are denoted with a lowercase g). These positions occur in a variety of secondary structural contexts: position 14 is in β-strand 1; positions 17−20 are in loop 1; positions 23 and 26 are in β-strand 2; position 30 is in loop 2; and position 33 is in β-strand 3 (Figure 2C).

In the subsequent discussion, we use the term glycosylation loosely to refer to both biological *N*-glycosylation and to the Asn to Asn−GlcNAc substitution used to generate the Pin WW variants in Figure 2A. However, it is important to note that this Asn to Asn−GlcNAc substitution differs from biological *N*-glycosylation in at least two ways. First, biological *N*-glycosylation appends a triantennary glycan to an Asn residue, whereas our approach uses the much smaller Asn−GlcNAc, which can be incorporated into chemically synthesized proteins using a commercially available protected amino acid (compare Figures 1 and 2B). Despite the smaller size of GlcNAc relative to the triantennary glycan, we hypothesized that the Asn to Asn−GlcNAc substitution would nevertheless have a significant effect on protein folding energetics. Such was the case previously for CD2ad, in which addition of a single GlcNAc residue stabilizes the protein by 2.0 kcal/mol.[45] Several spectroscopic studies of the conformations adopted by GlcNAc-modified glycopeptides,[26−28,30−33,35−39] along with computational modeling of glycosylated Src SH3 domains,[46] provide additional support for this hypothesis.

A second difference is that biological *N*-glycosylation only occurs at Asn residues that are located within an Asn−Xxx−Thr/Ser sequon (with Thr or Ser at the +2 position, two residues closer to the C-terminus of the protein than the modified Asn), whereas our chemical approach allows us to examine the effects of the Asn to Asn−GlcNAc substitution at any position in the Pin WW domain, whether or not Thr or Ser is present at the +2 position. This approach does not address the possibility that interactions between the *N*-glycan and the Thr/Ser side-chain at the +2 position might contribute to the effect of the Asn to Asn−GlcNAc substitution on glycoprotein folding. However, GlcNAc−Thr interactions were not observed previously in several conformational studies of GlcNAc-modified glycopeptides.[35−39] Furthermore, excluded volume effects (which we anticipated would be the major consequence of the Asn to Asn−GlcNAc substitution) should not depend on the exact identity of side-chains near the glycosylation site. Consequently, we chose not to modify the wild-type side-chain at the +2 position in each Asn or Asn−GlcNAc-containing variant.

We hoped that the comparison between the Pin WW variants with Asn and Asn−GlcNAc at each site would generate insights into the general thermodynamic and kinetic effects of glycosylation on naïve protein sequences. We also hoped that the differences between the predicted and experimental thermodynamic and kinetic results for each site would provide insights into the factors that allow glycosylation to accelerate folding and stabilize the folded state relative to the denatured ensemble.

We used the simplified native topology-based model[46,74] to predict the thermodynamic and kinetic effects of the Asn or Asn−GlcNAc substitutions at each of the nine selected positions. We also measured the kinetic and thermodynamic consequences of these substitutions experimentally using variable temperature circular dichroism and laser temperature jump kinetic experiments,[55,75] and compared variants containing Asn−GlcNAc at each position with corresponding variants,

(74) Levy, Y.; Cho, S. S.; Onuchic, J. N.; Wolynes, P. G. *J. Mol. Biol.* **2005**, *346*, 1121–1145.
(75) See the Supporting Information for details.

Table 3. Experimentally Measured and Computationally Predicted Folding Rates for Pin WW Variants Having Either Asn or Asn−GlcNAc at the Indicated Positions[a]

structural context	protein	residue at indicated position	measured folding rate[b] (10^3 s^{-1})	(k_f [Asn–GlcNAc])/(k_f [Asn]) measured	predicted[c]
β-strand 1	**14**	Asn	—[d]	—[d]	2
	14g	Asn−GlcNAc	—[d]		
loop 1	**17**	Asn	10.6 ± 0.7	0.76 ± 0.06	3.6
	17g	Asn−GlcNAc	8.1 ± 0.3		
	18	Asn	10.3 ± 0.6	0.78 ± 0.05	3.7
	18g	Asn−GlcNAc	8.1 ± 0.3		
	19	Asn	10.4 ± 0.4	0.80 ± 0.06	2.8
	19g	Asn−GlcNAc	8.3 ± 0.5		
	20	Asn	7.9 ± 0.3	*1.13 ± 0.06*	*2.4*
	20g	Asn−GlcNAc	9.0 ± 0.4		
β-strand 2	**23**	Asn	—[d]	—[d]	1.1
	23g	Asn−GlcNAc	—[d]		
	Pin WW	Asn	11.5 ± 0.9	—[d]	0.9
	26g	Asn−GlcNAc	—[d]		
loop 2	**Pin WW**	Asn	11.5 ± 0.9	*1.15 ± 0.11*	*3.4*
	30g	Asn−GlcNAc	13.3 ± 0.6		
β-strand 3	**33**	Asn	14.5 ± 1.0	*0.59 ± 0.11*	*0.8*
	33g	Asn−GlcNAc	8.7 ± 1.5		

[a] Variants for which experimental observations agree with computational predictions are italicized. [b] Measured folding rates at 55 °C (328.15 K) were calculated on the basis of relaxation data from laser temperature jump experiments on 100 μM solutions of each Pin WW domain variant in 20 mM sodium phosphate buffer (pH 7; see the Supporting Information for details). Uncertainties represent the standard error in folding rates. [c] Predicted folding rate ratios at the indicated positions were calculated on the basis of the all-atom native-topology model at the calculated melting temperature of the corresponding nonglycosylated Asn-containing Pin WW variant (in contrast with the measured folding rate ratios, which are all at 55 °C). [d] The folding kinetics of peptides **14**, **14g**, **23**, **23g**, and **26g** could not be analyzed via laser temperature-jump experiments due to their low thermal stability.

which contain only Asn. Tables 1 and 2 summarize the thermodynamic results. Glycosylation is stabilizing to Pin WW at just two of the nine positions. At position 20 in loop 1, the melting temperature T_m increases by 1.8 °C when Asn (**20**) is replaced by Asn−GlcNAc (**20g**). Similarly, at position 30 in loop 2, the T_m increases by 1.3 °C when Asn (**Pin WW**) is replaced by Asn−GlcNAc (**30g**). The increase in thermodynamic stability upon glycosylation at each of these two positions is consistent with the computational predictions and is similar to the increase observed previously upon glycosylation of the naïve helical protein Im7 (in which T_m increases by 0.6 °C).[37] However, the magnitude of the change ($\Delta\Delta G \approx -0.1$ kcal/mol at 55 °C) is ∼20-fold smaller than was observed upon adding GlcNAc to human CD2ad ($\Delta\Delta G = -2.0$ kcal/mol).[45]

Glycosylation is destabilizing to Pin WW at the other seven positions. The computational model accurately predicts this destabilizing result at three of the seven positions. At position 23 in β-strand 2, replacing Asn (**23**) with Asn−GlcNAc (**23g**) results in a dramatic loss in stability with T_m decreasing by ∼20 °C. Glycosylation at positions 26 (compare **Pin WW** with **26g**) and 33 (compare **33** with **33g**) is similarly destabilizing, with T_m decreasing by ∼50 and 4.4 °C, respectively. The fact that these destabilizing substitutions occur at positions that make a large number of contacts with nearby residues in the computational model[75] agrees with the rough inverse correlation between number of native contacts and glycosylation-induced increases in protein stability previously observed in silico with Src SH3.[46] This result suggests that adding a bulky GlcNAc residue to positions 23, 26, and 33 disrupts important stabilizing intramolecular interactions in the native state structural ensemble.

However, the location, structure, connectivity, and dynamics of a particular site do not always provide sufficient information to accurately predict whether glycosylation at that site will stabilize the protein. For example, the computational model predicts that the Asn to Asn−GlcNAc substitution will be stabilizing to Pin WW at position 14 in β-strand 1, and at positions 17, 18, and 19 in loop 1. In fact, we observe the opposite. T_m decreases by ∼20 °C upon glycosylation at position 14 (compare **14** with **14g**); at positions 17, 18, and 19, T_m decreases by 0.8 °C (compare **17** with **17g**), 2.4 °C (compare **18** with **18g**), and 2.9 °C (compare **19** with **19g**), respectively, upon glycosylation. The destabilizing effect of glycosylation at positions 17, 18, and 19 in loop 1 is particularly noteworthy because loop 1 is relatively flexible and is extended away from the tightly packed core of the Pin WW domain; such a location seems ideally suited for stabilization via glycan-based excluded volume effects. These results suggest that glycan-based excluded volume effects and the structure, connectivity, and dynamics of a particular position provide an incomplete understanding of how glycosylation at that position will change the thermodynamics of protein folding.

The kinetic data present a similar picture. Table 3 shows folding rates at 55 °C for Pin WW variants that have either Asn or Asn−GlcNAc at selected positions, along with computationally predicted changes in the folding rate at each position upon glycosylation. Table 4 shows unfolding rates at 55 °C for Pin WW variants that have either Asn or Asn−GlcNAc at selected positions, along with computationally predicted changes in unfolding rate at each position upon glycosylation. In Tables 3 and 4, the computationally predicted folding and unfolding rate ratios for each mutant were calculated at the predicted T_m of the corresponding Asn-containing variant.

The modest stabilizing effect of the Asn to Asn−GlcNAc substitution at positions 20 and 30 appears to be a result, in part, of an increased folding rate. Glycosylation at position 20 (compare **20** with **20g**) increases the folding rate ∼1.1-fold (Table 3). Glycosylation at position 30 (compare **30** with **30g**) has a similar effect. These small folding rate increases agree with the predictions of the computational model and could be consistent with a small amount of denatured-state destabilization as a consequence of glycosylation. However, the decreased unfolding rate of **20g** relative to **20** (also predicted by the model) could indicate that glycosylation at position 20 actually stabilizes the folding transition state and native state simultaneously. The

Table 4. Experimentally Measured and Computationally Predicted Unfolding Rates for Pin WW Variants Having Either Asn or Asn−GlcNAc at the Indicated Positions[a]

structural context	protein	residue at indicated position	measured unfolding rate[b] (10^3 s^{-1})	(k_u [Asn–GlcNAc])/(k_u [Asn])	
				measured	predicted[c]
β-strand 1	**14**	Asn	−[d]	−[d]	0.50
	14g	Asn−GlcNAc	−[d]		
loop 1	**17**	Asn	11.0 ± 1.0	*0.86 ± 0.10*	*0.58*
	17g	Asn−GlcNAc	9.4 ± 0.6		
	18	Asn	8.9 ± 0.6	1.10 ± 0.11	0.56
	18g	Asn−GlcNAc	9.8 ± 0.7		
	19	Asn	8.6 ± 0.5	1.22 ± 0.12	0.33
	19g	Asn−GlcNAc	10.5 ± 0.8		
	20	Asn	10.5 ± 0.7	*0.88 ± 0.08*	*0.45*
	20g	Asn−GlcNAc	9.3 ± 0.6		
β-strand 2	**23**	Asn	−[d]	−[d]	0.77
	23g	Asn−GlcNAc	−[d]		
	Pin WW	Asn	7.9 ± 0.8	−[d]	4.3
	26g	Asn−GlcNAc	−[d]		
loop 2	**Pin WW**	Asn	7.9 ± 0.8	0.96 ± 0.13	0.70
	30g	Asn−GlcNAc	7.6 ± 0.7		
β-strand 3	**33**	Asn	97.7 ± 13.9	0.96 ± 0.31	2.4
	33g	Asn−GlcNAc	93.8 ± 27.3		

[a] Variants for which experimental observations agree with computational predictions are italicized. [b] Measured unfolding rates at 55 °C (328.15 K) were calculated on the basis of relaxation data from laser temperature jump experiments on 100 μM solutions of each Pin WW domain variant in 20 mM sodium phosphate buffer (pH 7; see the Supporting Information for details). Uncertainties represent the standard error in unfolding rates. [c] Predicted unfolding rate ratios at the indicated positions were calculated on the basis of the all-atom native-topology model at the calculated melting temperature of the corresponding nonglycosylated Asn-containing Pin WW variant (in contrast with the measured unfolding rate ratios, which are at 55 °C). [d] The unfolding kinetics of peptides **14**, **14g**, **23**, **23g**, and **26g** could not be analyzed via laser temperature-jump experiments due to their low thermal stability.

destabilizing effect of glycosylation at position 33 (compare **33** with **33g**) appears to come only from a reduced folding rate, and not from a change to unfolding rate (whereas the model predicted a decreased folding rate and an increased unfolding rate).

As was the case for the thermodynamic results, the glycosylation-induced changes to folding rate at positions 17 (compare **17** with **17g**), 18 (compare **18** with **18g**), and 19 (compare **19** with **19 g**) do not agree with computational predictions. Whereas glycosylation at each of these positions was predicted to increase the folding rate, we observe the opposite (Table 3). The observed changes to unfolding rate at positions 18 and 19 are similarly inconsistent with the computational predictions. Whereas the Asn to Asn−GlcNAc subsitution at these positions was predicted to decrease unfolding rate, we observe either no change or a slight increase in unfolding rate. In contrast, glycosylation at position 17 appears to decrease unfolding rate slightly, which does agree with the computational predictions.

Discussion

Although we have focused here on comparing Pin WW variants that have either Asn or Asn−GlcNAc at a given site, it should be noted that replacing wild-type residues with Asn is often destabilizing to Pin WW (Table 1), especially at position 14 in β-strand 1, 23 in β-strand 2, and 33 in β-strand 3 (where the wild-type residues are Arg, Tyr, and Gln, respectively; Figure 2C). This loss of stability may reflect the inability of Asn to form favorable contacts with nearby residues as efficiently as do the wild-type side chains; it may also reflect the lower β-strand propensity of Asn relative to Arg, Tyr, and Gln.[76] Glycosylation at each of these positions results in even further decreases in stability, possibly as a result of rigidifying unfavorable Asn side-chain conformations.[43]

(76) Muñoz, V.; Serrano, L. *Proteins: Struct., Funct., Genet.* **1994**, *20*, 301–311.

The computational model successfully predicts the sign of the effect of glycosylation on the thermodynamic stability of Pin WW at positions 20, 23, 26, 30, and 33, although the predicted and experimental magnitudes are quite different in some cases. The model fails to predict accurately the sign of the thermodynamic effect of glycosylation at positions 14, 17, 18, and 19. The predictions appear to be most accurate at positions where the Asn to Asn−GlcNAc substitution is strongly destabilizing. Asn to Asn−GlcNAc substitution was predicted to be destabilizing at positions 23, 26, and 33, presumably because these positions are highly structured in the folded state of wild-type Pin WW and each make a large number of contacts with nearby residues. Our observations agree with these predictions in each case, suggesting that glycosylation at highly structured locations disrupts important stabilizing interactions in the native state structural ensemble via generic glycan-based excluded volume effects.

In contrast, the model is less accurate at predicting positions where the Asn to Asn−GlcNAc substitution is stabilizing to Pin WW. Of the six sites predicted by the model to be stabilized by glycosylation (positions 14, 17, 18, 19, 20, and 30), only two are actually stabilized (positions 20 and 30). The discrepancy between experiment and computation is particularly notable at positions 17, 18, and 19 in flexible loop 1, which is relatively far removed from potentially destabilizing steric clashes with side-chains in the tightly packed core of the Pin WW domain, and seems ideally suited for the stabilizing glycan-based excluded volume effects that we hypothesized would be so significant.

One potential explanation for this discrepancy in loop 1 is that the computational model is based on the NMR structure of wild-type Pin WW[51] and assumes that the native states of our Asn- or Asn−GlcNAc-containing variants have the same three-dimensional structure, an assumption that may not reflect reality in atomic detail. The similar shape of the CD spectra of each of our Asn- and Asn−GlcNAc-containing variants suggests that

their three-dimensional structures are similar,[75] but our melting temperature data show that glycoproteins **17g**, **18g**, and **19g** are each slightly less stable than are proteins **17**, **18**, and **19**. It is possible that these small changes in thermodynamic stability are accompanied by structural rearrangements in either the native state or the denatured ensemble for which the computational model does not account. If so, calculations based on the wild-type Pin WW NMR structure might be unable to predict accurately the effect of glycosylation at those positions. The discrepancy between computational predictions and experimental observations at positions 17, 18, and 19 could reflect the presence of glycosylation-associated structural rearrangements that prevent the formation of favorable interactions between Asn and other protein side-chain or backbone groups. These rearrangements would themselves be evidence that glycan-based excluded volume effects play a less significant role in changing glycoprotein folding energetics at unstructured positions than we originally hypothesized.

A related possibility is that glycan-based excluded volume effects generally destabilize proteins (by disrupting important native state interactions) unless there are specific favorable interactions between the saccharide and protein side-chain or backbone groups. For example, the observed increased stability and increased folding rate of **20g** relative to **20**, and of **30g** relative to **30**, could be the result of simultaneous transition state and native state stabilization (rather than destabilization of the denatured ensemble), reflecting the presence of favorable glycan−protein contacts at these positions. Similarly, the observed destabilizing effect of glycosylation at positions 17, 18, and 19 in loop 1 could reflect the unanticipated absence of favorable GlcNAc−protein interactions at these positions. The results of our study show that generic glycan-based excluded volume effects do not provide a sufficient explanation for the effect of the Asn to Asn−GlcNAc substitution at flexible positions and suggest that specific, context-dependent GlcNAc−protein interactions play a more significant role than we originally hypothesized.

Conclusions

While the basis for the differences between the predicted and experimental data can be debated, co-consideration of the experimental and computational data allows definitive conclusions to be drawn. First, the stabilizing effects of glycosylation on the naïve Pin WW domain, when observed, were an order of magnitude smaller than those reported for the evolved glycoprotein CD2ad (−2.0 kcal/mol), suggesting that specific, evolved protein−glycan contacts play an important role in mediating the unusually large effects of glycosylation on the folding energetics of CD2ad, and are likely important in other glycoproteins as well. Second, increased thermodynamic stabilization and increased folding rate (whether from denatured ensemble destabilization or from transition state and native state stabilization) are apparently not general, context-independent consequences of introducing a glycosylation site into a naïve protein, even when the glycosylation site is placed within a flexible region such as a loop, where excluded volume effects would be predicted to be most influential. Finally, factors other than glycan-based excluded volume effects (accompanied by consideration of local structure, connectivity and dynamics) strongly influence whether or not glycosylation will be stabilizing to Pin WW at positions in flexible loops. These factors could include significant structural rearrangements of Pin WW upon glycosylation and/or the presence or absence of explicit stabilizing interactions between GlcNAc and protein side-chain or backbone groups. The hypothesis that specific GlcNAc–protein side-chain interactions play an important role in stabilizing proteins by *N*-glycosylation is currently being explored.

Experimental Section

Protein Synthesis. WW domain variants were synthesized as C-terminal acids employing a solid-phase peptide synthesis approach using a standard Fmoc Nα protecting group strategy either manually or via a combination of manual and automated methods. Amino acids were activated by 2-(1*H*-benzotriazole-1-yl)-1,1,3,3-tetramethyluronium hexafluorophosphate (HBTU, purchased from Advanced ChemTech) and *N*-hydroxybenzotriazole hydrate (HOBt, purchased from Advanced ChemTech). Fmoc-Gly-loaded Novasyn TGT resin and all Fmoc-protected α-amino acids with acid-labile side-chain protecting groups were purchased from EMD Biosciences, including the glycosylated amino acid Fmoc−Asn(Ac_3GlcNAc)−OH (*N*-α-Fmoc-N-*β*-[3,4,6-tri-*O*-acetyl-2-(acetylamino)-deoxy-2-*β*-glucopyranosyl]-L-asparagine).[72,73] Piperidine and *N*,*N*-diisopropylethylamine (DIEA) were purchased from Aldrich, and *N*-methyl pyrrolidinone (NMP) was purchased from Applied Biosystems.

Acid-labile side-chain protecting groups were globally removed, and peptides were cleaved from the resin by stirring the resin for ∼4 h in a solution of phenol (0.5 g), water (500 μL), thioanisole (500 μL), ethanedithiol (250 μL), and triisopropylsilane (100 μL) in trifluoroacetic acid (TFA, 8 mL), and peptides were precipitated from the TFA solution by addition of diethyl ether (∼45 mL). Acetate protecting groups were subsequently removed from the GlcNAc 3-, 4-, and 6-hydroxyl groups in Asn(GlcNAc)-containing peptides by hydrazinolysis, as described previously.[77] Peptides were purified by preparative reverse-phase HPLC on a C18 column using a linear gradient of water in acetonitrile with 0.2% v/v TFA. Peptides were identified by matrix-assisted laser desorption/ionization time-of-flight spectrometry (MALDI-TOF), and purity was determined by analytical HPLC.[75]

Circular Dichroism Spectroscopy. Circular dichroism (CD) measurements were made with an Aviv 62A DS circular dichroism spectrometer, using quartz cuvettes with a 0.1 cm path length. Peptide solutions were prepared in 10 mM sodium phosphate buffer, pH 7, and peptide concentrations were determined spectroscopically on the basis of tyrosine and tryptophan absorbance at 280 nm in 6 M guanidine hydrochloride + 20 mM sodium phosphate (ε_{Trp} = 5690 M^{-1} cm^{-1}, ε_{Tyr} = 1280 M^{-1} cm^{-1}).[78] CD spectra were obtained by monitoring molar ellipticity from 340 to 200 nm, with 5 s averaging times. Variable temperature CD data were obtained by monitoring molar ellipticity at 227 nm from 0.2 to 98.2 at 2 °C intervals, with 90 s equilibration time between data points and 30 s averaging times. Variable temperature CD data were fit to equations for two-state thermally induced unfolding transitions (in cases where clear pre- and post-transition baselines were apparent), and T_m and other relevant thermodynamic parameters were obtained for each peptide as parameters of the fit.[75]

Laser Temperature Jump Experiments. Relaxation times following a rapid laser-induced temperature jump of ∼12 °C were measured by monitoring Trp fluorescence of a 100 μM solution of each Pin WW domain peptide in 20 mM sodium phosphate (pH 7) using a nanosecond laser temperature jump apparatus, as described previously.[55,79−81] The fluorescence decay of a Trp residue in each WW variant was monitored following a laser-induced temperature

(77) Ficht, S.; Payne, R. J.; Guy, R. T.; Wong, C.-H. *Chem.-Eur. J.* **2008**, *14*, 3620–3629.
(78) Edelhoch, H. *Biochemistry* **1967**, *6*, 1948–1954.
(79) Ballew, R. M.; Sabelko, J.; Reiner, C.; Gruebele, M. *Rev. Sci. Instrum.* **1996**, *67*, 3694–3699.
(80) Ballew, R. M.; Sabelko, J.; Gruebele, M. *Proc. Natl. Acad. Sci. U.S.A.* **1996**, *93*, 5759–5764.
(81) Ervin, J.; Sabelko, J.; Gruebele, M. *J. Photochem. Photobiol., B* **2000**, *54*, 1–15.

jump at each of several temperatures. The time evolution of the decay traces was best fit to a monoexponential equation, yielding the observed rate constants at each temperature as parameters of the fits. The observed rate constants obtained in the temperature jump experiments were combined with equilibrium constants from the variable temperature CD experiments to calculate unfolding and folding rates.[75]

Native Topology Model Calculations. We applied a native topology-based model[46,74] (Gō model) to study the folding of Pin WW domain variants with Asn or Asn−GlcNAc at various positions of interest. All local, secondary, and tertiary native contacts between amino acids are represented by the Lennard-Jones potential without any discrimination between the various chemical types of the interactions. The Hamiltonian of the system and its parameters can be found elsewhere.[82,83] The simulations were preformed using the GROMACS software package.[83] Multiple trajectories were simulated using the Langevin equation with friction constant of 0.5 ps^{-1}. The trajectories were analyzed using the weighted histogram analysis method (WHAM)[84] to study the folding thermodynamics. The GlcNAc-conjugated variants were built using the Glyprot web server.[85] Additional details can be found in the Supporting Information.

Acknowledgment. We thank S. R. Hanson and E. K. Culyba for helpful discussions. This work was supported in part by the Skaggs Institute for Chemical Biology, the Lita Annenberg Hazen Foundation, and by National Institutes of Health (NIH) grant GM51105 to J.W.K. and E.T.P. J.L.P. was supported in part by an NIH postdoctoral fellowship (F32 GM086039). A.D. and M.G. were supported by National Science Foundation grant MCB 1019958. Y.L. was supported by the Kimmelman Center for Macromolecular Assemblies and the Israel Science Foundation. Y.L. holds the Lillian and George Lyttle Career Development Chair.

Supporting Information Available: Complete experimental methods, compound characterization, circular dichroism data, and laser temperature jump kinetic data. This material is available free of charge via the Internet at http://pubs.acs.org.

JA106896T

(82) Whitford, P. C.; Noel, J. K.; Gosavi, S.; Schug, A.; Sanbonmatsu, K. Y.; Onuchic, J. N. *Proteins* **2009**, *75*, 430–41.
(83) Noel, J. K.; Whitford, P. C.; Sanbonmatsu, K. Y.; Onuchic, J. N. *Nucleic Acids Res.* **2010**, *28*, W657−W661.
(84) Kumar, S.; Bouzida, D.; Swendsen, R. H.; Kollman, P. A.; Rosenberg, J. M. *J. Comput. Chem.* **1992**, *13*, 1011–1021.
(85) Bohne-Lang, A.; von der Lieth, C. W. *Nucleic Acids Res.* **2005**, *33*, W214–W219.